

Discrete momentum representation of the Lippmann-Schwinger equation and its application to electron-molecule scattering

Martin Poláček

Faculty of Philosophy and Science, Silesian University at Opava, Bezručovo nám. 13, 746 01 Opava, Czech Republic

Michael Juřek, Marek Ingr, and Petr Čářský

J. Heyrovský Institute of Physical Chemistry, Academy of Sciences of the Czech Republic, 18223 Prague 8, Czech Republic

Jiří Horáček

Faculty of Mathematics and Physics, Charles University, V Holešovičkách 2, 18000 Prague 8, Czech Republic

(Received 17 November 1997; revised manuscript received 26 July 1999; published 9 February 2000)

We present a way of using numerical quadrature in momentum space for solving the three-dimensional Lippmann-Schwinger equation. The integration is performed in spherical coordinates. Test calculations show that the quadrature is well suited for the electron-molecule scattering problems. Sample results of elastic scattering of electrons are presented for the empirical Yukawa potential and *ab initio* Hartree-Fock potential of the hydrogen and methane molecules.

PACS number(s): 34.80.Bm

I. INTRODUCTION

Progress in calculations of electron-molecule collisions has been recently reviewed in several books and review articles (see, for example, Refs. [1] and [2]). Recent variational treatments of electron-molecule collisions (see, for example, Refs. [3–5]) usually use Gaussian-type functions as the variational basis set. Although the use of Gaussians in bound-state calculations has become a routine task, their utilization in scattering problems is not so simple. One needs a large set of diffuse functions to represent properly all the operators appearing in the variational functional. Moreover, the *S*-matrix Kohn method requires additional continuum functions with correct asymptotic behavior. The choice of the resulting set is connected with some uncertainty and may lead to linear dependency. For these reasons, it is desirable to separate basis functions used for the construction of the Hartree-Fock potential and those appearing in the solution of the scattering equations. We attempted this by developing the cubic grid Gaussian basis sets (CGGBS) [6–10] consisting of *s*-type Gaussians centered at the points of a regular cubic lattice. The basic construction principle of the CGGBS—the best fit of the plane wave—allows the expression of the Green's function in a separable form and the acquisition of *T* elements by simple inversion of the Lippmann-Schwinger (LS) equation. Unfortunately, this method suffers from two main disadvantages: without semi-empirical adjustment it yields infinite diagonal elements of the Green's function, and the interaction potential matrix expressed in CGGBS becomes nearly singular at lower energies.

To overcome these problems we decided to modify the method originally proposed by Walters [11] who used a numerical quadrature in **k** space to solve the Lippmann-Schwinger equation. To point out the formal analogy with the discrete variable representation, we refer to the proposed method as to the discrete momentum representation (DMR) method. The method leads to a matrix equation for scattering amplitudes similar to that in the *T*-matrix expansion [12].

The discrete set of quadrature vectors in the **k** space may be considered as a basis set which allows to represent the *T*-operator matrix once the molecular potential is available in any standard basis set.

II. THEORY

A. Standard numerical solution of the Lippmann-Schwinger equation

The problem of solving the Lippmann-Schwinger equation [13]

$$T(E) = U + UG_0(E)T(E), \quad (1)$$

where *U* stands for double of the potential, is encountered in many branches of physics and chemistry and its efficient solution is of a vital importance. The standard way of tackling this problem consists in carrying out the partial-wave expansion of all the quantities and solving a coupled set of one-dimensional partial wave LS equations of the following type

$$t_l(p, p'; E) = u_l(p, p') + \frac{1}{\pi} \int_0^\infty \frac{u_l(p, k) t_l(k, p'; E) k^2 dk}{k^2 - k'^2 + i\epsilon} \quad (2)$$

in momentum space [14]. This equation is singular (singular integrand and infinite integration range) and special attention must be paid to the correct treatment of the singularity. There exist several more or less satisfactory ways of treating the singularity of the integral kernel (see, for example, Refs. [15–19]). Here we quote a widely used approach [19] consisting of the following. The infinite integration range (0; ∞) is reduced to (−1; 1) by means of the transformation

$$x = \frac{k - k_0}{k + k_0}, \quad (3)$$

where

$$k_0 = \sqrt{\frac{2\mu E}{\hbar^2}}, \quad (4)$$

which sets the kernel singularity to the middle of the integration range, $x=0$. For computation of the resulting integrals which are of the type

$$P \int_{-1}^1 \frac{f(x)dx}{x}, \quad (5)$$

the use of $2n$ -point Gaussian rules is recommended, since not only do they have maximum degree of exactness, but because of the symmetry they also integrate exactly the function $1/x$ [20]. It is also possible to subtract the singularity [14] by writing

$$P \int_{-1}^1 \frac{f(x)dx}{x} = \int_{-1}^1 \frac{f(x)-f(0)}{x} dx. \quad (6)$$

Then also $(2n+1)$ -point Gaussian rules may be used. The symmetric distribution of quadrature nodes with respect to zero permits us to neglect the subtraction term. The partial wave LS equation is then solved for a series of angular momentum quantum number l and the cross sections obtained by summing contributions from all partial waves. This approach is very efficient provided the number of contributing partial waves is low. This is true for very low-energy electrons and spherical targets. At higher energies and for heavier particles the number of partial waves increases rapidly and soon the method becomes impractical.

B. Essence of the discrete momentum representation

We propose a different method which avoids the partial-wave expansion and which is directly applicable to non-spherical targets. The idea is to solve the LS equation in the full three-dimensional momentum space:

$$\langle \mathbf{k}_1 | T | \mathbf{k}_2 \rangle = \langle \mathbf{k}_1 | U | \mathbf{k}_2 \rangle + \int \frac{\langle \mathbf{k}_1 | U | \mathbf{k} \rangle \langle \mathbf{k} | T | \mathbf{k}_2 \rangle d\mathbf{k}}{k_0^2 - k^2 + i\epsilon}. \quad (7)$$

To do so, we express the LS equation in spherical coordinates in the \mathbf{k} space and treat separately the radial and angular integrations. Let us write the T -matrix element as

$$\langle \mathbf{k}_1 | T | \mathbf{k}_2 \rangle = \langle \mathbf{k}_1 | U | \mathbf{k}_2 \rangle + \int_0^\infty \frac{k^2 f(\mathbf{k}_1, \mathbf{k}_2; k) dk}{k_0^2 - k^2 + i\epsilon}, \quad (8)$$

where the function $f(\mathbf{k}_1, \mathbf{k}_2; k)$ is defined as

$$f(\mathbf{k}_1, \mathbf{k}_2; k) = \int d\Omega \langle \mathbf{k}_1 | U | k\mathbf{n}(\Omega) \rangle \langle k\mathbf{n}(\Omega) | T | \mathbf{k}_2 \rangle, \quad (9)$$

and the symbol $\mathbf{n}(\Omega)$ stands for the unit vector in the direction Ω . The solution of Eq. (8) may be in principle performed by the numerical technique described in the previous subsection. An efficient method for angular numerical quadrature was developed by Lebedev [21] and has been applied to problems in electronic-structure [22] and electron-scattering theories [23].

Using this numerical quadrature, we solve a set of linear algebraic equations and we obtain the T matrix on a three-dimensional grid in momentum space. For this approach, to be efficient, the total number of mesh points must be low. It can be achieved by restricting the radial integration region by using the following substitution:

$$k = k_0 \frac{a + bx}{a - bx}. \quad (10)$$

With respect to Eq. (3), the transformation (10) diminishes considerably the extent of the numerical quadrature by cutting off the high-energy region. Without this cutoff it is difficult to reach a convergence of the numerical procedure. The transformation (10) also cuts off the low-energy region, though this is less justifiable than the cutoff of the high-energy region. However, the parameters a and b may be set so that the disregarded region is small and its exclusion does not affect the result. By numerical tests we chose $a = 10.3333$ and $b = 9.6667$ as default values since they represent a good compromise between the computational effort (given by the number of quadrature points) and accuracy (see Sec. IID for details). The transformation (10) gives a symmetric distribution of the quadrature nodes and the subtraction term in Eq. (6) vanishes.

Application of both the radial and angular quadratures to Eq. (7) converts it to the matrix form

$$\mathbf{T} = \mathbf{U} + \mathbf{U} \mathbf{G}_0^+ \mathbf{T}, \quad (11)$$

in which the matrix elements are defined as

$$T_{qj,pi} = \langle k_q \mathbf{n}_j | T | k_p \mathbf{n}_i \rangle, \quad (12)$$

$$V_{qj,pi} = \langle k_q \mathbf{n}_j | V | k_p \mathbf{n}_i \rangle, \quad (13)$$

$$(G_0^+)_{qj,pi} = \begin{cases} -\delta_{qp} \delta_{ji} w_i k_0 i/2 & \text{if } p=0, \\ \delta_{qp} \delta_{ji} \frac{2abw_p w_i k_p^2 k_0}{(a-bx_p)^2 (k_0^2 - k_p^2)} & \text{if } p \neq 0. \end{cases} \quad (14)$$

Subscripts p, q and i, j are indices of nodes in the radial and angular quadratures, respectively, w is the weight, and x_p is defined by Eq. (10). V is the interaction potential and $U = 2V$. The matrix \mathbf{T} may be obtained by the matrix inversion

$$\mathbf{T} = (\mathbf{1} - \mathbf{U} \mathbf{G}_0^+)^{-1} \mathbf{U}. \quad (15)$$

A peculiar feature of the DMR approach is that we do not obtain directly the scattering amplitude for an *a priori* selected scattering angle, but for a set of discrete angular coordinates given by the numerical quadrature. The scattering amplitude for a particular scattering angle can be obtained by an additional computational procedure (see Sec. IIE).

C. Scattering of electrons on molecular targets

Calculations of electron-molecule collisions are usually performed with the use of the optical potential in static-exchange approximation

TABLE I. Dependence of the differential (DCS) and integral (ICS) cross sections of the elastic e -CH₄ scattering on the extent of the integration range. a , b —parameters of Eq. (10); k_{\min} , k_{\max} —lower and upper limit of the integration range; N_{rad} , N_{ang} —number of radial and angular quadrature points necessary for the convergence.

E (eV)	a	b	k_{\min} (a.u.)	k_{\max} (a.u.)	N_{rad}	N_{ang}	DCS [$\text{\AA}^2/\text{sr}$]			ICS (\AA^2)
							0°	90°	180°	
5	10.67	9.33	0.040	9.09	21	110	2.73	0.882	2.67	17.16
	10.5	9.5	0.030	12.12	21	110	2.64	0.892	2.4	16.6
	10.4	9.6	0.024	15.15	21	110	2.51	0.89	2.2	16.0
	10.33	9.67	0.020	18.19	25	110	2.48	0.88	2.15	15.7
20	11.00	9.00	0.121	12.12	21	146	10.50	0.495	1.436	16.49
	10.67	9.33	0.081	18.19	23	194	10.56	0.40	1.44	16.6
	10.50	9.50	0.061	24.25	25	194	10.59	0.40	1.42	16.7
	10.40	9.60	0.048	30.31	25	194	10.58	0.40	1.41	16.7
	10.33	9.70	0.040	36.37	29	194	10.59	0.41	1.40	16.7

$$V = V_s + V_{\text{ex}}. \quad (16)$$

The static part includes electrostatic interaction of the scattered electron with the charge density

$$\rho(\mathbf{r}) = -\sum_A Z_A \delta(\mathbf{r} - \mathbf{R}_A) + 2 \sum_i |\phi_i(\mathbf{r})|^2, \quad (17)$$

where Z_A , \mathbf{R}_A , and ϕ_i have their usual meaning of nuclear charges, atomic positions, and occupied molecular orbitals. The corresponding matrix element is expressed as

$$\langle \mathbf{k}_1 | V_s | \mathbf{k}_2 \rangle = \frac{4\pi}{K^2} \int e^{i\mathbf{k} \cdot \mathbf{r}} \rho(\mathbf{r}) d\mathbf{r}, \quad (18)$$

where $\mathbf{K} = \mathbf{k}_2 - \mathbf{k}_1$. Using second-order Taylor expansion for the exponential in Eq. (18) one can show that the last expression diverges for the targets with nonzero dipole moment at $K = 0$, whereas for systems with zero dipole moment the term becomes undefined. Since the forward V_s element is used only for integration and represents a zero-measure set, we can replace it by a point very close to $K = 0$. In the limit $K \rightarrow 0$ the forward Coulombic term yields the following formula,

$$\langle \mathbf{k} | V_s | \mathbf{k} \rangle = -\frac{2\pi}{k^2} \mathbf{k}^T \mathbf{M} \mathbf{k}, \quad (19)$$

where \mathbf{M} is the molecular second moment.

Finally, let us substitute for charge density of a closed shell target molecule from Eq. (17) and apply the linear combination of atomic orbitals expansion of molecular orbitals. The Coulombic matrix elements (18) in a nonforward direction become

$$\langle \mathbf{k}_1 | V_s | \mathbf{k}_2 \rangle = \frac{4\pi}{K^2} \left(-\sum_A Z_A e^{i\mathbf{k} \cdot \mathbf{R}_A} + \sum_\alpha \sum_\beta P_{\alpha\beta} \left\langle \mathbf{k}_1 \alpha \left| \frac{1}{r_{12}} \right| \mathbf{k}_2 \beta \right\rangle \right). \quad (20)$$

The elements of density matrix $P_{\alpha\beta}$ can be used also to calculate second moments. The exchange integrals may be evaluated in a similar manner

$$\langle \mathbf{k}_1 | V_{\text{ex}} | \mathbf{k}_2 \rangle = -\frac{1}{2} \sum_\alpha \sum_\beta P_{\alpha\beta} \left\langle \mathbf{k}_1 \alpha \left| \frac{1}{r_{12}} \right| \beta \mathbf{k}_2 \right\rangle, \quad (21)$$

and no special treatment is required for diagonal elements.

Packages for Hartree-Fock calculations use almost exclusively Gaussian basis sets. The formulas for hybrid Coulombic and exchange integrals are available in the literature [12,24–26].

D. Test of the truncated radial integration

In this section we comment on setting the constants a and b in Eq. (10). A pair of the constants a and b was chosen, which defines the integration range. For this integration range the calculations of the differential cross section were performed with increasing number of both the radial and angular quadrature mesh points, until the convergence was reached. Then the integration range was extended and a converged result was calculated again. This procedure was repeated so many times, until the result was stable. The constants a and b so obtained were accepted as standard values for all other calculations. These tests were done on the methane molecule with the molecular valence double ζ basis set [27]. The results for 5 and 20 eV are summarized in Table I.

E. Averaging over the molecular orientation

The results for electron scattering on molecules in the gas phase should account for random orientation of molecular targets. This fact requires an additional procedure to obtain differential cross sections averaged over molecular coordinates. As is usual [23], we keep the molecular target fixed and integrate the differential cross section over the pairs of \mathbf{k} vectors with a fixed scattering angle. The procedure is performed in the following manner. Around each vector from the angular set we assume a circle on the sphere with the

TABLE II. Differential cross sections (in $\text{\AA}^2/\text{sr}$) of elastic scattering of 1-eV electrons on the Yukawa potential. The results for different numbers of radial quadrature nodes (N) are compared with those obtained by partial-wave expansion (PWE). The number of angular quadrature nodes has been set to 38.

Scatt. angle (deg)	$N=5$	$N=7$	$N=9$	$N=11$	$N=15$	PWE
0.00	0.3969	0.3946	0.3939	0.3938	0.3937	0.3936
35.26	0.3658	0.3639	0.3632	0.3631	0.3630	0.3629
54.74	0.3296	0.3281	0.3274	0.3273	0.3273	0.3271
70.53	0.2971	0.2960	0.2953	0.2952	0.2951	0.2950
90.00	0.2587	0.2580	0.2573	0.2573	0.2572	0.2571
109.47	0.2262	0.2258	0.2251	0.2251	0.2250	0.2249
125.26	0.2054	0.2053	0.2047	0.2046	0.2046	0.2045
144.74	0.1873	0.1874	0.1867	0.1867	0.1866	0.1866
180.00	0.1747	0.1749	0.1743	0.1742	0.1742	0.1741

radius k_0 . The radius of the circle corresponds to the scattering angle. By numerical integration along this circle we obtain the averaged differential cross section for a particular \mathbf{k} vector. This is performed consecutively for all vectors from the angular set and the final value of the differential cross section is obtained by averaging the values calculated for individual \mathbf{k} vectors. The procedure is general and may be used for any set of scattering angles. However, it is profitable to select scattering angles given by the angular quadrature, because such a selection reduces the number of the

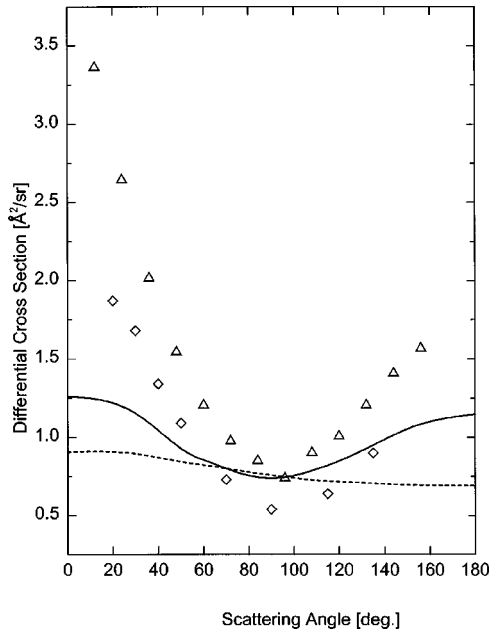


FIG. 1. Angular dependence of the differential cross section of elastic electron scattering on H_2 at 5 eV. The calculated results were obtained with 11 radial and 38 angular points. The lines representing results obtained for 13, 15, and 17 radial points and higher numbers of angular points are indistinguishable from the presented line. The dashed line represents the static result without inclusion of the exchange term. The experimental data are taken from Refs. [28] (squares) and [29] (triangles).

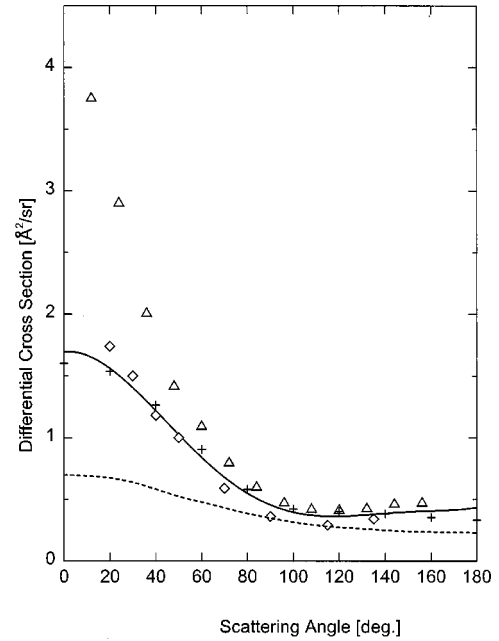


FIG. 2. Angular dependence of the differential cross section of elastic electron scattering on H_2 at 10 eV. See Fig. 1 for details. The crosses represent results of static-exchange calculations of Ref. [32].

U -matrix elements needed in the numerical integration on the circles. Presently we are working on a more efficient averaging procedure.

III. RESULTS AND DISCUSSION

As the first test of the radial and angular quadratures described in this paper we calculated angular dependence of the

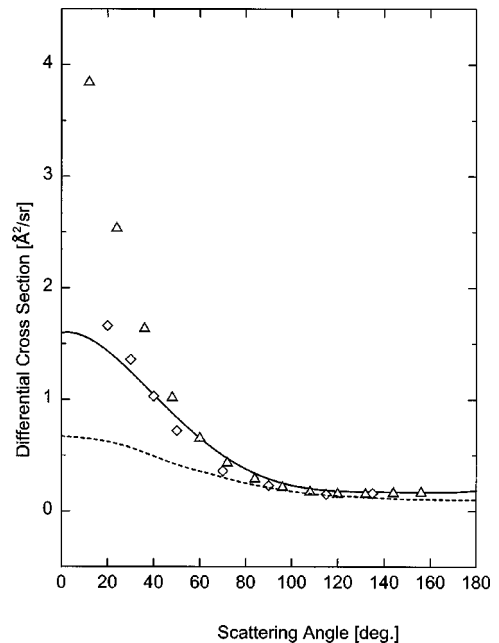


FIG. 3. Angular dependence of the differential cross section of elastic electron scattering on H_2 at 15 eV. See Fig. 1 for details.

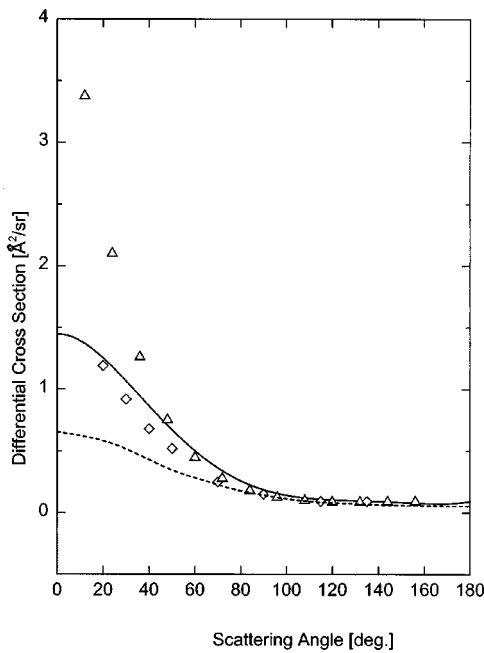


FIG. 4. Angular dependence of the differential cross section of elastic electron scattering on H₂ at 20 eV. See Fig. 1 for details.

differential cross section for elastic electron scattering on the Yukawa potential

$$V = \frac{e^{-r}}{r}. \tag{22}$$

The calculated elastic cross sections at 1 eV compared with those obtained by partial wave expansion are shown in Table II. We present results for five sets of radial quadrature nodes. Because of spherical symmetry of the potential, the calculated cross sections depend only very little on the number of

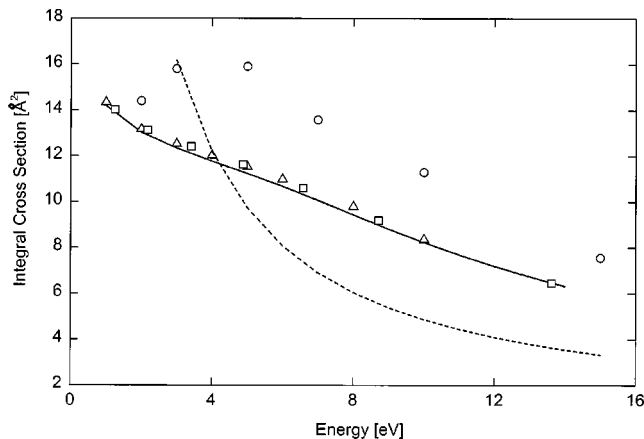


FIG. 5. Elastic integral cross section for *e*-H₂ scattering. The solid line represents results obtained by use of the quadrature with 11 radial and 38 angular points. Higher quadratures give lines that are indistinguishable from the presented line. The dashed line represents the static result without inclusion of the exchange term. The experimental data (circles) are taken from Ref. [29]. The triangles and squares represent the results of static-exchange calculations of Refs. [31] and [32], respectively.

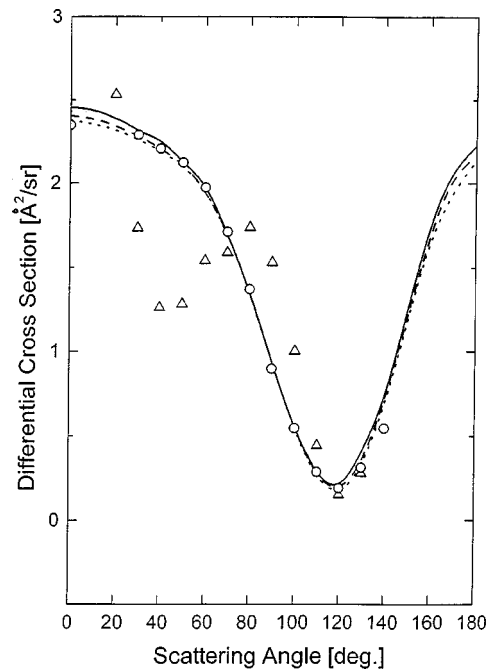


FIG. 6. Angular dependence of the differential cross section of elastic electron scattering on the methane molecule at 5 eV. The calculated results obtained by different numbers of angular points are represented as follows: 86, dotted line; 110, long dashes; 146, solid line. The experimental data are taken from Ref. [30] (triangles). The circles represent the results of static-exchange calculations of Ref. [33]. The static results are out of scale in this figure.

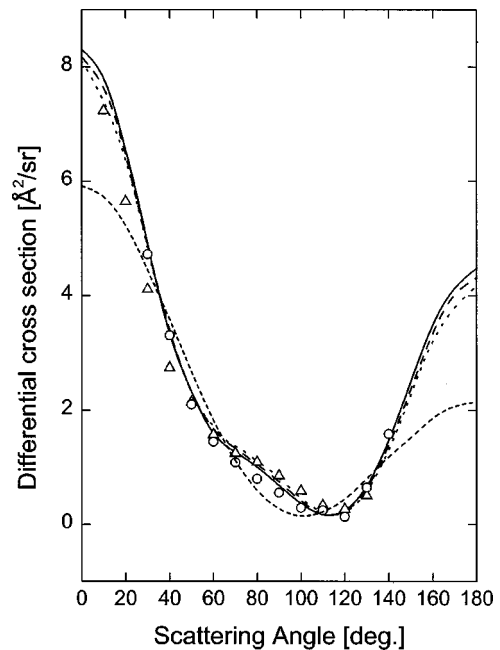


FIG. 7. Angular dependence of the differential cross section of elastic electron scattering on the methane molecule at 10 eV. See Fig. 6 for details. The dashed line represents the static result without inclusion of the exchange term.

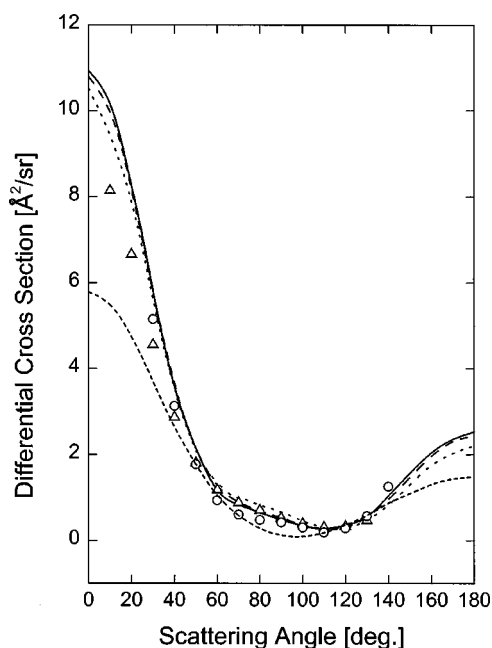


FIG. 8. Angular dependence of the differential cross section of elastic electron scattering on the methane molecule at 15 eV. See Figs. 6 and 7 for details.

angular nodes, and it is not necessary to apply Lebedev quadratures with more than 38 points. As can be seen in Table II, the DMR approach yields results exact to four digits.

In order to show the applicability of the DMR approach to real molecular systems, we calculated the cross sections of elastic electron scattering on hydrogen and methane molecules. Since the present version of our computer code allows only calculations in the static-exchange approximation, the polarization effects are not taken into account. For both H_2 and CH_4 the standard valence double ζ basis set [27] has been used for construction of the Hartree-Fock potential (16). The calculated cross sections for the elastic electron scattering on H_2 are presented in Figs. 1–4 along with two sets of experimental data. The angular quadrature set with 38 points is large enough in this case, and the extension of the angular set does not change the results. The curves in each one of Figs. 1–4 represent results obtained with different numbers of radial points ranging from 11 to 17. The minimal radial set with 11 points is large enough to represent the converged results. The absence of polarization contributions to the potential causes well-known underestimation of the calculated cross section near the forward direction. As can be seen in Fig. 5, the calculated cross section of elastic e - H_2 scattering follows closely the results of two other approaches [31,32]. Since the resulting integral cross section is mostly affected by near-forward contributions and no polarization effects have been introduced in the calculations, the calculated values differ significantly from the experimental ones. In all figures we also present the static results (i.e., cross sections obtained without the exchange potential), suggested for future comparison with other techniques.

The second example, dependence of the cross section of the elastic electron scattering on the methane molecule,

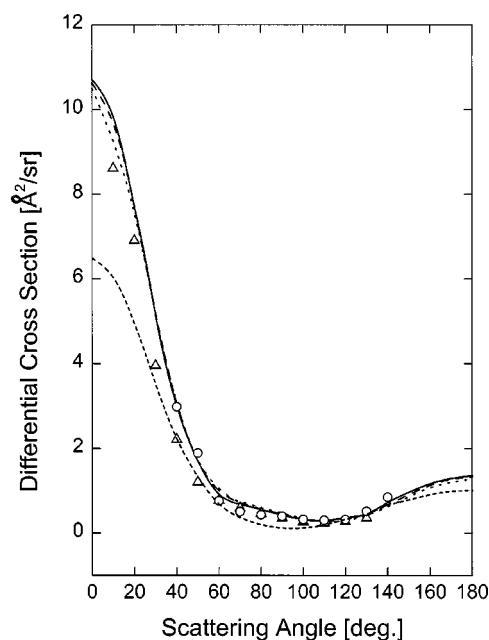


FIG. 9. Angular dependence of the differential cross section of elastic electron scattering on the methane molecule at 20 eV. See Figs. 6 and 7 for details.

shows good convergence of the results with the increasing size of the angular set. The calculated differential cross sections for three angular sets are plotted in Figs. 6–9. The number of radial nodes has been set to 21 in all three cases. As it is seen, DMR calculations provide results very close to experimental data. The agreement is worse for 5 eV because of the neglect of polarization effects.

IV. CONCLUSION

We presented a method for the calculation of the cross sections of electron-molecule collisions based on a numerical quadrature applied to the Lippmann-Schwinger equation in momentum space. The suggested distribution of quadrature nodes maintains a relatively high precision of the numerical procedure. The method seems to be feasible for calculations of electron scattering on polyatomic molecules. Since the size of the resulting set of linear equations is not related to the number of atoms of the molecule, the presented treatment could be suitable for economical calculations of electron-molecule scattering on personal computers.

At the present time the method is restricted to calculations of elastic electron or positron scattering cross sections on nonpolar targets. Further extension to polar systems as well as the treatment of various types of inelastic collisions and inclusion of polarization effects will be the subject of subsequent papers.

ACKNOWLEDGMENTS

This work was supported by Grant No. 203/99/0839 of the Grant Agency of the Czech Republic. The computer time provided by Supercomputing Center Brno is gratefully acknowledged.

- [1] *Computational Methods for Electron-Molecule Collisions*, edited by W. M. Huo and F. A. Gianturco (Plenum, New York, 1995).
- [2] *Novel Aspects of Electron-Molecule Collisions*, edited by K. H. Becker (World Scientific, Singapore, 1998).
- [3] T. N. Rescigno, B. H. Lengsfeld III, and C. W. McCurdy, in *Modern Electronic Structure Theory*, edited by D. R. Yarkony (World Scientific, Singapore, 1995), Pt. I.
- [4] C. Winstead and V. McKoy, in *Modern Electronic Structure Theory* (Ref. [3]), Pt. II.
- [5] M.-T. Lee, L. M. Brescansin, and L. E. Machado, Phys. Rev. A **59**, 1208 (1999).
- [6] P. Čársky, V. Hrouda, and J. Michl, Int. J. Quantum Chem. **53**, 419 (1995).
- [7] P. Čársky, V. Hrouda, and J. Michl, Int. J. Quantum Chem. **53**, 431 (1995).
- [8] P. Čársky, V. Hrouda, J. Michl, and D. Antic, Int. J. Quantum Chem. **53**, 437 (1995).
- [9] V. Hrouda, M. Polášek, P. Čársky, and J. Michl, Theor. Chim. Acta **89**, 401 (1994).
- [10] P. Čársky, V. Hrouda, M. Polášek, D. E. David, D. Antic, and J. Michl, J. Phys. Chem. A **101**, 3754 (1997).
- [11] H. R. J. Walters, J. Phys. B **4**, 437 (1971).
- [12] T. N. Rescigno, C. W. McCurdy, and V. McKoy, Phys. Rev. A **11**, 825 (1975).
- [13] R. G. Newton, *Scattering Theory of Waves and Particles* (Springer, New York, 1982).
- [14] S. K. Adhikari and K. L. Kowalski, *Dynamical Collision Theory and Its Applications* (Academic, Boston, 1991).
- [15] M. Harada, R. Tamagaki, and H. Tanaka, Prog. Theor. Phys. **33**, 1003 (1966).
- [16] M. Harada, Prog. Theor. Phys. **38**, 353 (1967).
- [17] M. I. Haftel and F. Tabakin, Nucl. Phys. **A158**, 1 (1970).
- [18] W. Glöckle, *The Quantum Mechanical Few-Body Problem* (Springer, New York, 1983).
- [19] I. H. Sloan, J. Comput. Phys. **3**, 332 (1968).
- [20] G. Monegato, Computing **29**, 337 (1982).
- [21] V. I. Lebedev, Zh. Vychisl. Mat. Mat. Fiz. **16**, 293 (1976).
- [22] C. W. Murray, N. C. Handy, and G. J. Laming, Mol. Phys. **78**, 997 (1993).
- [23] C. Winstead and V. McKoy, Adv. Chem. Phys. **96**, 103 (1996).
- [24] D. K. Watson and V. McKoy, Phys. Rev. A **20**, 1474 (1979).
- [25] P. Čársky and M. Polášek, J. Comput. Phys. **143**, 266 (1998).
- [26] P. Čársky and T. Reschel, Collect. Czech. Chem. Commun. **63**, 1264 (1998).
- [27] T. H. Dunning, Jr. and P. J. Hay, in *Modern Theoretical Chemistry*, edited by H. F. Schaefer III (Plenum, New York, 1977), Vol. 3.
- [28] S. K. Srivastava, A. Chutjian, and S. Trajmar, J. Chem. Phys. **63**, 2659 (1975).
- [29] T. W. Shyn and W. E. Sharp, Phys. Rev. A **24**, 1734 (1981).
- [30] L. Boesten and H. Tanaka, J. Phys. B **24**, 821 (1991).
- [31] L. A. Collins, W. D. Robb, and M. A. Morrison, Phys. Rev. A **21**, 488 (1980).
- [32] T. L. Gibson, M. A. P. Lima, K. Takatsuka, and V. McKoy, Phys. Rev. A **30**, 3005 (1984).
- [33] M. A. P. Lima, T. L. Gibson, W. M. Huo, and V. McKoy, Phys. Rev. A **32**, 2696 (1985).